Surface-Wave Analysis in the Taipei Basin from Strong-Motion Data

Jen-Kuang Chung[1] and Tzay-Chyn Shin[1]

ABSTRACT

Fundamental-mode Love waves, with period ranging from 2 to 7 sec, were recorded by the dense strong-motion network in Taipei basin, during the June 5, 1994 Nanao earthquake. In the frequency-wavenumber spectra, the Love waves propagating in the direction from the epicenter to the basin were verified to be the principal phases in this period range. Using the interstation surface-wave inversion method, the shallow crustal structure beneath the basin was determined. Results show that the shear-wave velocities of 1 to 4 km deep layers are in the range from 2.1 to 2.4 km/sec. Accordingly, a lateral variation derived within the basin is evident.

(Key words: Love wave, Dispersion analysis, Structure inversion, Taipei basin)

1. INTRODUCTION

Study of the strong ground motion characteristics requires detailed knowledge of the effect of shallow geological structure on surface motion in the engineer-interest period range from one to ten seconds, because of the increasing number of high-rise buildings, long-spanned bridges, and other large-scale structures. The duration of strong ground motion, for example, is mostly responded to the shallower crustal S-wave velocity to be related with the propagation of surface waves. The estimation of ground motions in this long-period range has become an important aspect of seismic hazard mitigation.

Swanger and Boore (1978) mentioned that the long-period characteristics of ground motion are controlled not only by near surface soil condition, but also by the characteristics of the bedrock below. Yamanaka et al. (1989) made forward modeling of the 3 to 10 sec ground motions in the Kanto plain, Japan, during the western Nagano earthquake of 1984, with 2-D finite-difference method. They conclude that the configuration of sedimentary layers plays a crucial role in propagation and amplification of earthquake ground motions on basins. In the theoretical and numerical simulations, a well-determined layer structure is necessary for the prediction of strong ground motion when the fault rupture occurs near the target area (Vidale and Helmberger, 1988).

---

[1]Seismology Center, Central Weather Bureau, Taipei, Taiwan, ROC

Taipei City is a metropolis in northern Taiwan, which is located on a sediment-filled basin and is very near to the most active northeastern seismic belt. Two moderate Hualien earthquakes of May 20 (M_L=6.2) and November 14 (M_L=6.8), 1986, caused some damage on the buildings and killed 14 persons in the Taipei area; that occurred surprisingly about 110 km away from the source region. Similar cases happened in the September 19, 1985 Michoacan, Mexico earthquake which cause devastating destruction in Mexico City (Campillo et al., 1989) and also in the 1989 Loma Prieta earthquake to the Bay area of San Francisco (Hanks and Krawinkler, 1991; McGarr et al., 1991). In such an environment of thick soil layer overlying the hard rock, the short-period surface waves propagating over a distance compared to several times of focal depth are usually amplified to prolong the length of recording time of trigger-type accelerographs at the sites. Those records, therefore, contain enough information from the surface waves for inverting the shallow structure.

The subsurface stratigraphic structure of Taipei basin has been explored using geological boring, in-situ testing, geophysical prospecting, earthquake observation, and laboratory tests by Central Geological Survey since 1991. According to the results from the boreholes and reflection seismic surveys, the depth of deepest basement should be in the range from 400 m to 550 m (Wang et al., 1994, 1995; Teng et al., 1996). The velocity distribution of the Quaternary deposit above the basement has also been determined well (Hsieh et al., 1996; Wang, 1996). Using the tomographic inversion, the deeper structure has obtained in previous studies (Yeh and Tsai, 1981; Rau and Wu, 1995; Chen, 1995). However, their results are generally in large scale and cannot provide a fine description for the upper part of basement, which is the key factor for estimating the ground motion. On the basis that many strong-motion data are available in recent, the surface-wave method is becoming one of the ways to get more understanding in the shallow structure. For this reason, the purpose of this paper is to estimate the shear-wave velocity structure under the Taipei basin utilizing well-dispersed Love waves observed by the dense strong-motion network during the Nanao earthquake (M_L=6.2) of June 5, 1994. The data used here are the most complete sets of strong-motion records in Taipei area, since the big-size shallow depth event is seldom occurred in this region. The waves of period range from 2 to 7 sec, that can resolve the Tertiary basement down to about 4 km deep, are considered.

2. STRONG-MOTION DATA

2.1 TSMIP Network

The Taiwan Strong Motion Instrumentation Program (TSMIP), conducted by the Central Weather Bureau (CWB), has been in operation since July 1991 (Shin, 1993). Over 600 digital free-field accelerographs are deployed over nine metropolitans in Taiwan. The spacing between two adjacent stations is, on average, 2 km within the Taipei basin and 5 km in the other areas. Each station consists of a three-component force-balanced accelerometer, either an A-900 or IDS-3602, with a 16-bit resolution and a 96-db dynamic range. The full scale of recording system is ±2g. The net system response to acceleration is almost flat from DC to 50

Page	Mistake	Correction
886		
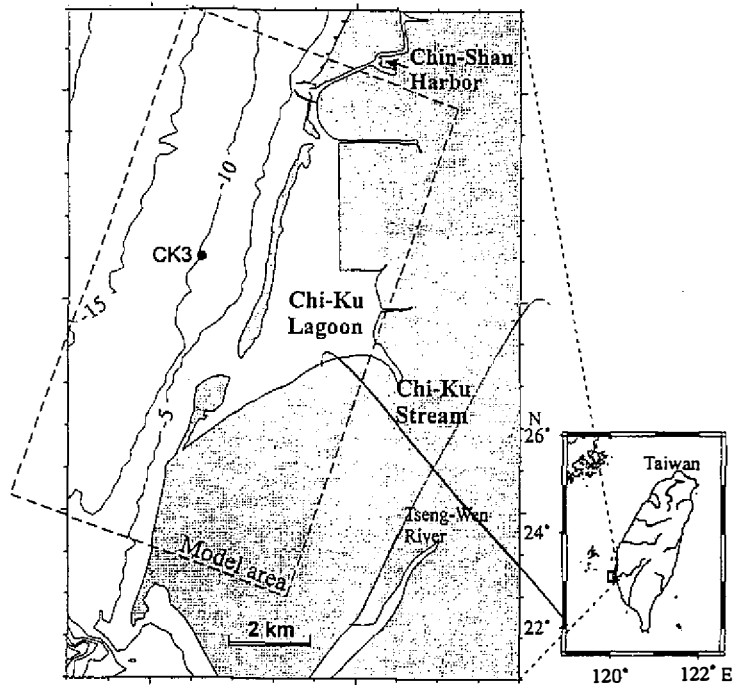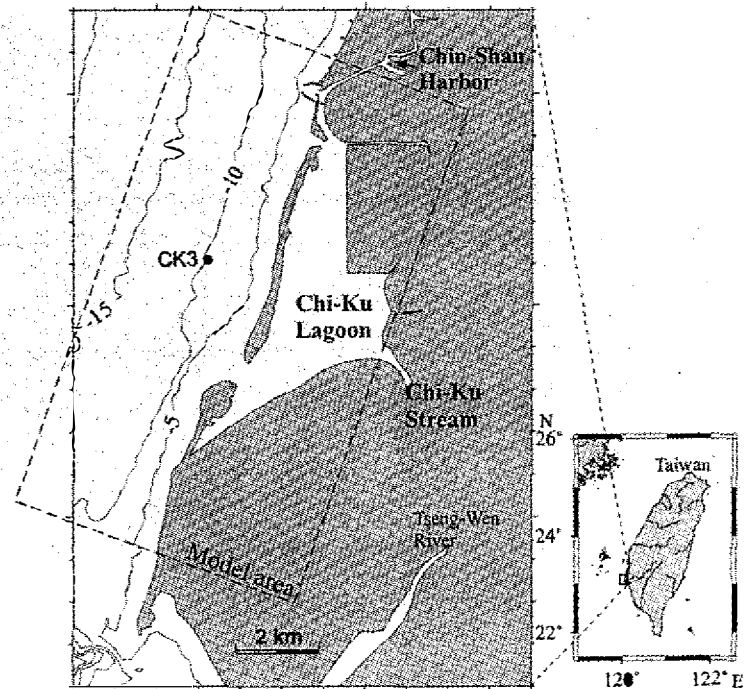
CASE (DYNE/CM²)	TIDE CONSTITUENT R(M³/S)		S/N		WIND STRESS
A	M2	2	0	0	
B	M2	1/2	0	0	
W	M2	2	1	0	
R	M2	2	0		200

CASE	TIDE CONSTITUENT	S/N	WIND STRESS (DYNE/CM²)	R(M³/S)
A	M2	2	0	0
B	M2	1/2	0	0
W	M2	2	1	0
R	M2	2	0	200

| 898 | Second line from the bottom… "瀉湖" | "潟湖" |

Page	Mistake	Correction
642		
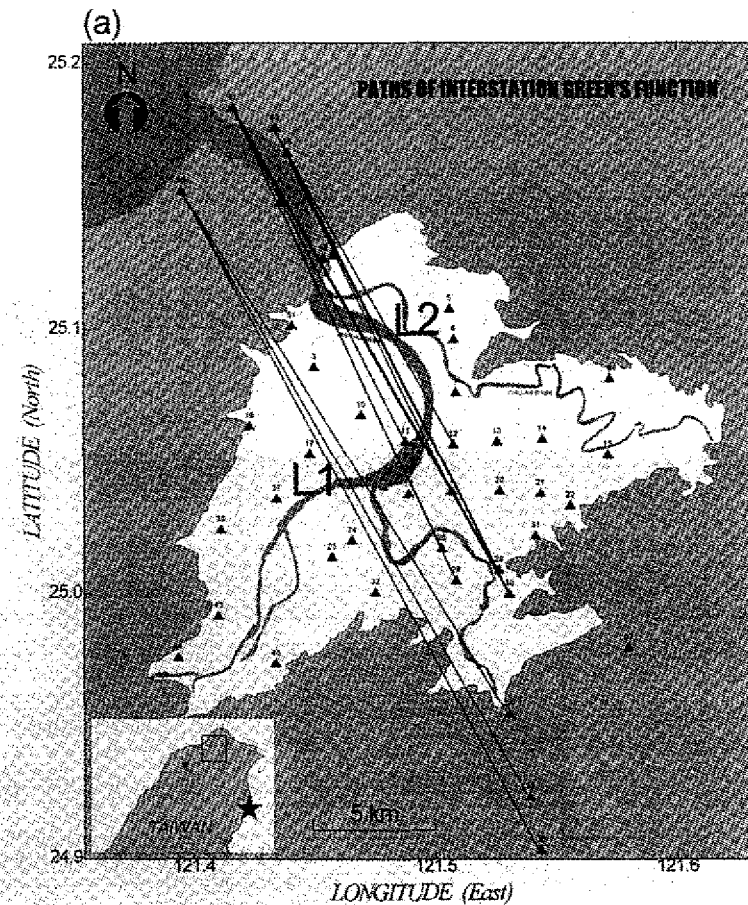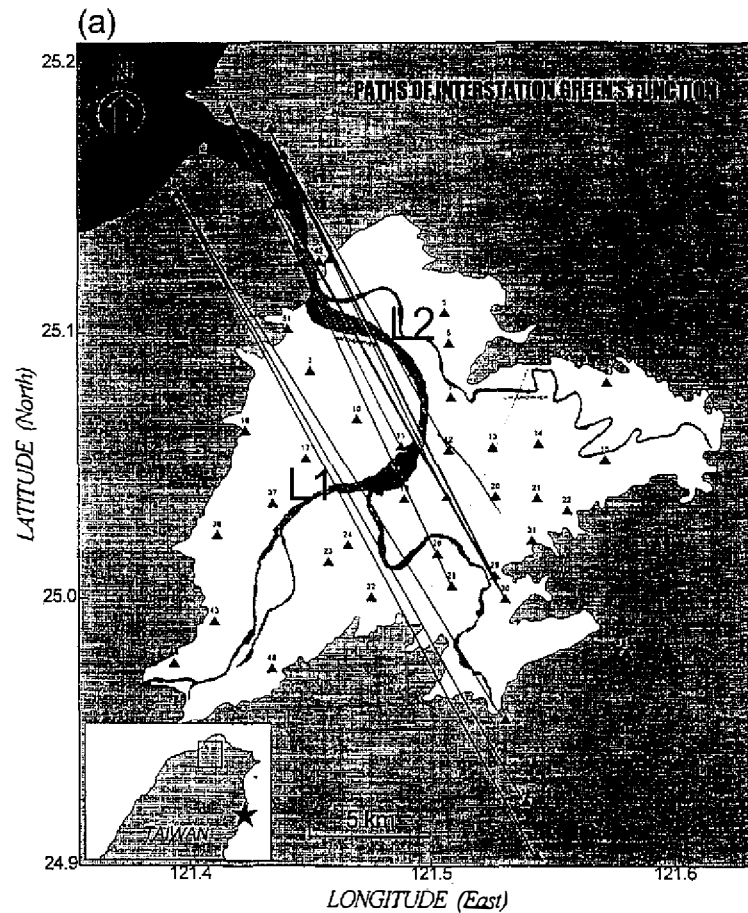
Hz. The basic specifications of the both types of instruments are the same, except the sampling rate.

2.2 Strong-Motion Data of 5 June 1994 Earthquake

The Nanao earthquake of June 5, 1994, with the mechanism of left-lateral strike-slip faulting in E-W direction (Shin, 1996), occurred in the northeastern Taiwan (epicenter location: 121.8°E, 24.46°N), which is about 70 km far away from the center of Taipei basin. The local magnitude is 6.2 in Richter scale determined by the CWB. The focal depth of the mainshock is 5 km. Most of the free-field strong-motion stations in Taipei area were triggered during this earthquake (Fig. 1). The overall ground shakings of intensity 4 (corresponding to the acceleration range from 25 to 80 gals) were observed. The low-frequency signals generally exist in the records following to the S-waves for all of the three components. Some of the E-W component accelerograms are shown in Fig. 2.

Based on the focal mechanism and the very shallow focal depth, significant surface waves should be observed in Taipei basin. To examine the characteristics of these lower-frequency wavetrains, the raw acceleration data are integrated to the velocity waveforms and are filtered to cut the frequency content lower than 0.1 Hz off in the frequency domain. The amplitudes of surface waves in the period range of 2 to 5 sec, therefore, become the dominant phases in the records. The distinct dispersive characteristic is shown, in each component of the record of every station, implying the existence of both of the Rayleigh wave and Love wave. The selected 43 records provide good opportunity to investigate the behavior of surface waves propagating within the Taipei basin, because of the dense distribution of stations and of the high S/N ratio in each observation.

Before the strong-motion data to be utilized for the wave-propagation study, the accuracy of initial recording time of the data must be concerned since there is no common-base timing system for the TSMIP free-field stations. Fortunately, the Global Positioning System (GPS) is equipped to calibrate the timing system of each A-900, except for the IDS-3602 with the number of station code below 25. A simple technique is performed for checking the recording time in this paper. All of the clear first motions are picked out from the vertical component, and then the calculated travel times are plotted versus the epicentral distances. These data represent an approximate linear relationship with an apparent P-wave velocity of 5.167 km/sec, except few IDS-3602 observations. The assumption, of the ignorance for the topographic and shallower geological effects on the travel time, is reasonable in this case. The recording time of those having large bias from the relationship is therefore calibrated to the 'true' one, which is closest to the time-to-distance line, by adding/subtracting integer seconds. The result is depicted in Fig. 3. The largest error may not exceed 0.3 sec after the correction, which could be ignored for the interest period range, based on the assumption.

2.3 F-K Analysis

Ray paths of short-period Love waves might be bent away from the direction toward the station due to the lateral structure variation (Teng and Qu, 1996). Phillips et al. (1993) also observed complicate 1-sec Love waves initiating from certain edges of the Kanto basin. In the

TAIPEI BASIN STRONG MOTION NETWORK
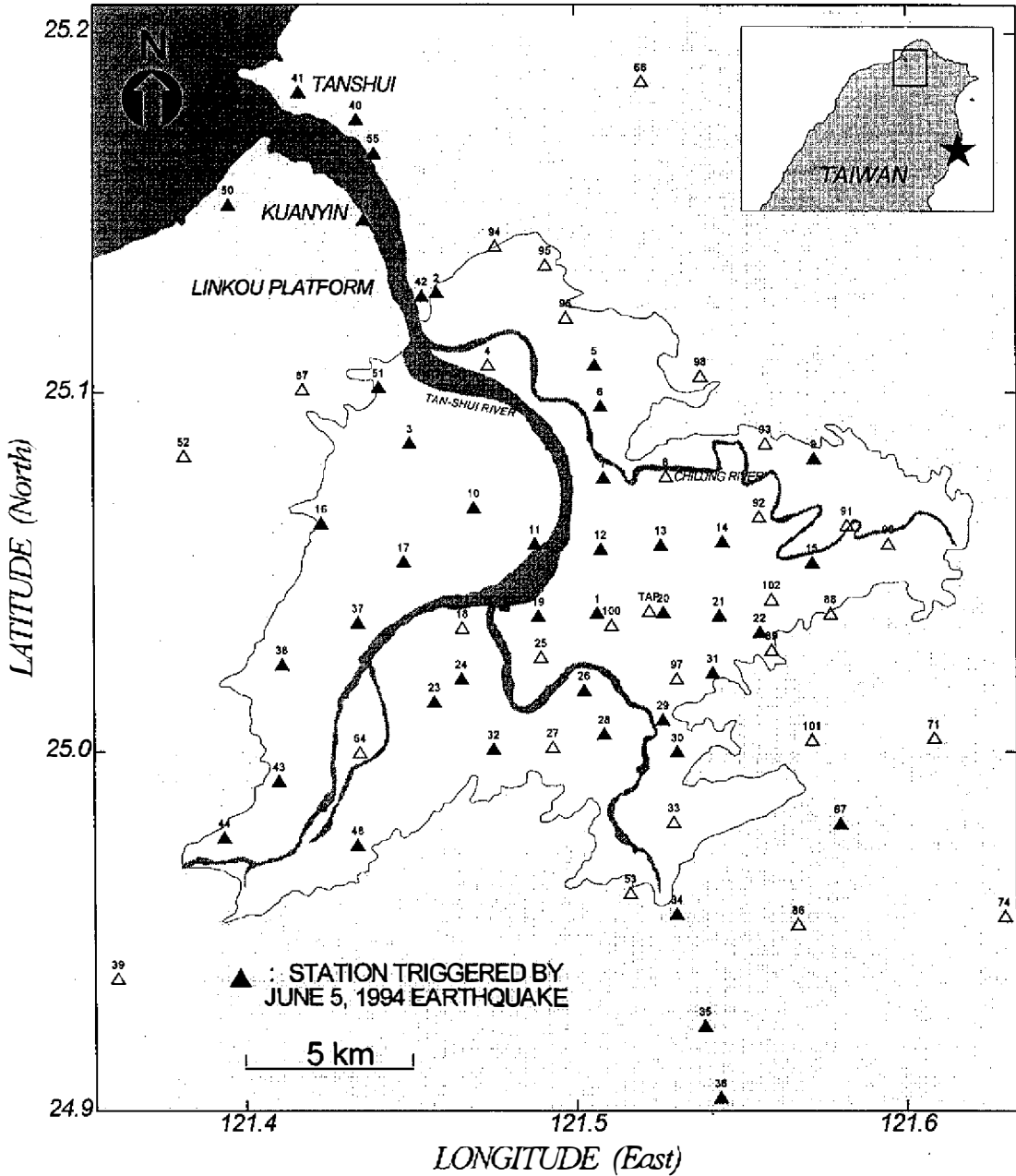
Fig. 1. Locations of the TSMIP network stations in Taipei area. Numbers indicate the station codes. The solid triangles denote the stations triggered during the June 5, 1994 earthquake (epicenter is represented by the asterisk in the upper panel).
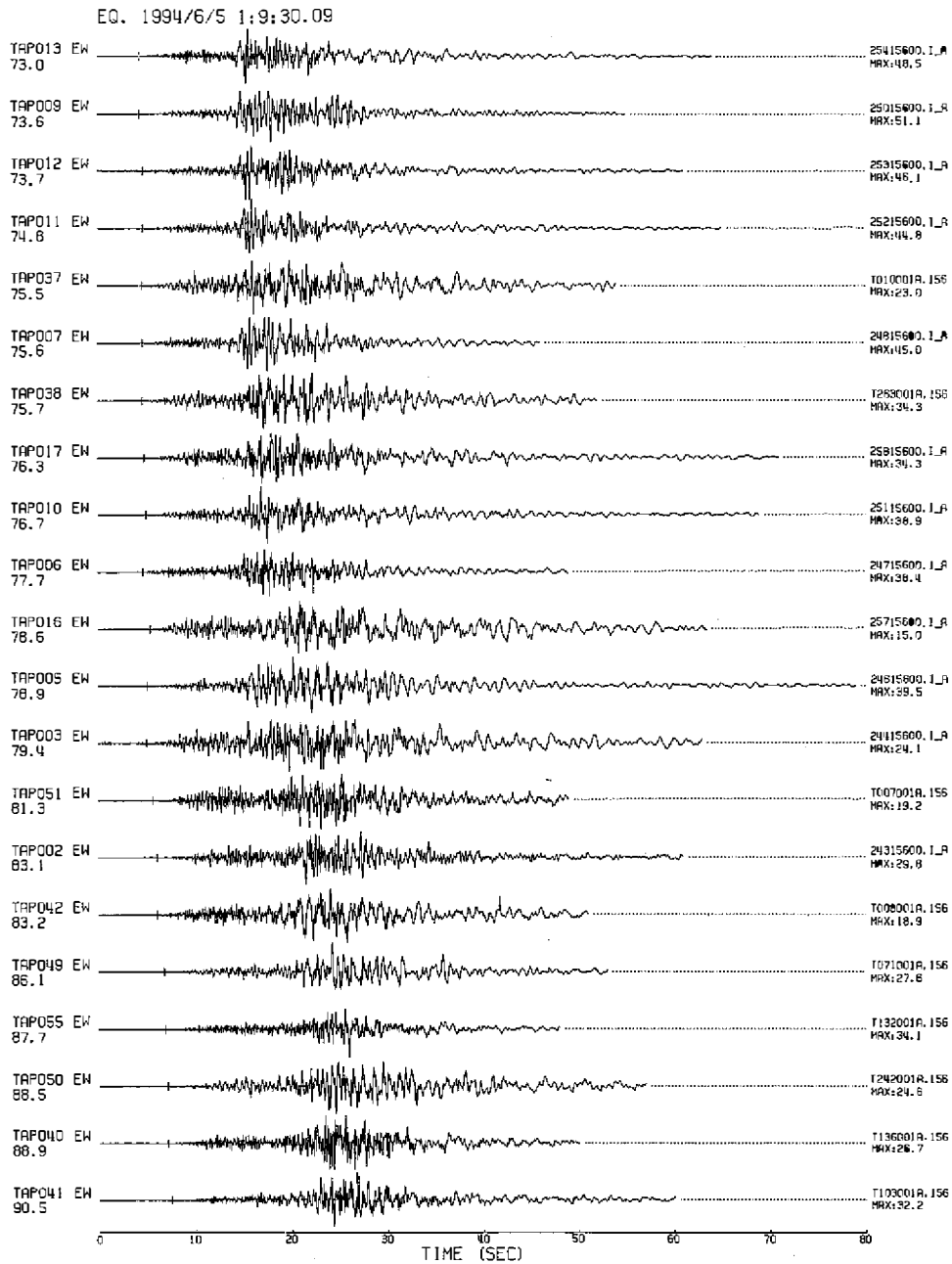
Fig. 2. Several E-W component strong-motion seismograms recorded during the 1994 earthquake. The amplitude is normalized in each seismogram. The peak ground accelerations (PGA) are also given in units of cm/sec/sec. Evident long-period waves can be observed after about 25 sec in each of waveforms.
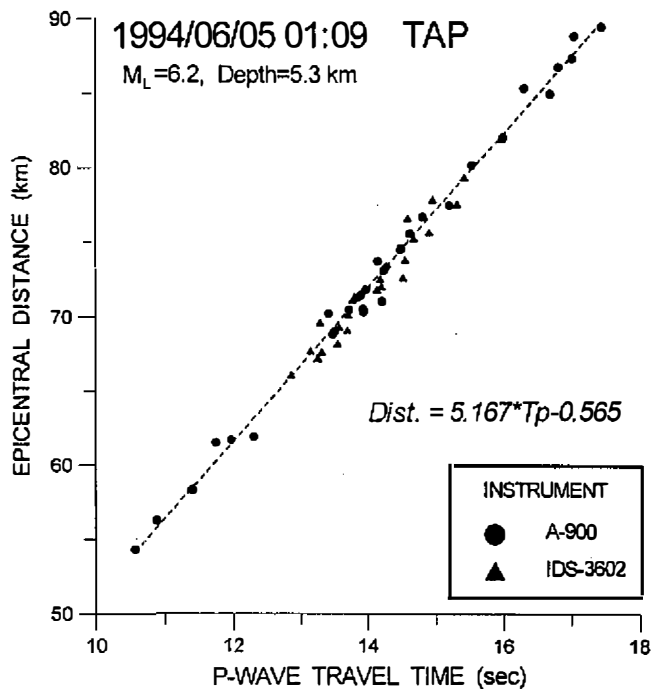
Fig. 3. Relationship between the epicentral distance and the P-wave travel time. The solid triangles denote the observations from IDS-3602, and the solid circles are from A-900. The slope of the dashed line, derived by least-square method, represents the apparent P-wave velocity in the Taipei basin.

similar case, the surface waves propagating in the Taipei basin are, at first, need to be identified their source in this paper. The time-space observations are thus transformed into the frequency-wavenumber (F-K) domain. The maximum-likelihood method (Capon, 1969) is used to analyze data from the 32 stations within the basin. The diameter of TSMIP network covering the whole Taipei basin is about 20 km, and consequently the resolution ability in wavenumber is 0.025. The minimum wavelength to be resolved is 4 km considering the 2-km station spacing. If the maximum wavenumber of surface waves is supposed as 0.2, the highest frequency of 0.5Hz can be resolved, with the propagation velocity of 2.5 km/sec.

For the six different frequencies of 0.15Hz, 0.2Hz, 0.25Hz, 0.3Hz, 0.4Hz, and 0.5Hz, respectively, the records with the length of about 30 seconds followed to shear-waves are analyzed. Each of records is divided into 2 to 7 windows with the width of twice of the interested period. Figure 4 shows the F-K spectra for the E-W component records. The dominant energy propagating in the azimuth of 333°, which is in the direction from the epicenter to the center of Taipei basin, is consistently observed for the analyzed frequencies. The apparent velocities are in the range from 2.1 to 2.6 km/sec. Another energy source from the northeastern direction of basin is also detected at a frequency below 0.3Hz. This observation could be due to the scattering from the edge of basin of the primary surface waves, with slightly lower

E-W Component
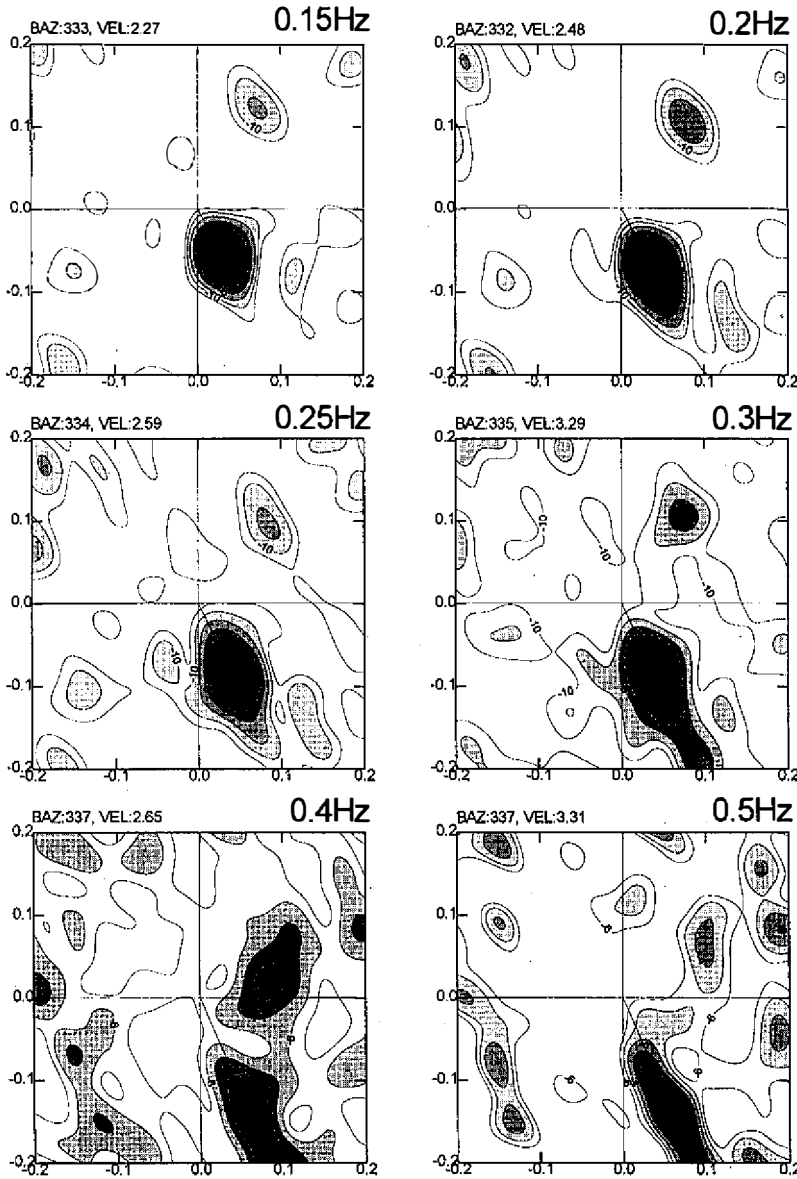
Fig. 4. Frequency-wavenumber spectra, for 0.15 Hz, 0.2 Hz, 0.25 Hz, 0.3 Hz, 0.4 Hz, and 0.5 Hz, derived from the TSMIP records of Taipei basin for the June 5, 1994 earthquake. The numbers on contours indicate the signal power (in decibels). The highest amplitude arrival is shown with the connection to the plot origin. Note the arrival from the southeast direction appearing as the principal phase on all the frequencies.

velocity than the 'major' signal. Overall, the scattered waves can be ignored for the surface-wave dispersion analysis because of their relative small amplitude. On the other hand, the significant scattered waves observed in each of three components, approximately from the eastern side of basin, may cause some interference on dispersion analysis when the 0.4-0.5Hz waves are considered. The effect on the dispersion analysis by the scattered energy will be discussed in the later section of this paper.

3. SURFACE-WAVE ANALYSES

For the purposes of understanding the characteristics of surface waves and of obtaining the S-wave velocity structure beneath the Taipei basin, fundamental-mode Love waves of the period range from 2 to 7 seconds are taken into account according to the results from the F-K analyses. Due to the dense distribution of strong-motion stations spread in and around the Taipei basin, the two-station phase-velocity method was employed for determining the interstation group- and phase-velocity dispersions. This method has the advantage of eliminating the uncertain source term. Various schemes for this method have been proposed (Bloch and Hales, 1968; Taylor and Toksoz, 1982; Dean and Keller, 1991). The Wiener deconvolution filtering in frequency domain is used in this study to obtain the phase velocities of the interstation Green's functions. Before taking the cross-spectra between near-station records and far-station records, fundamental-mode Love waves are extracted using phase-matching iteration (Herrin and Goforth, 1977). This approach avoids the interference from the higher-modes and multipath signals mentioned in previous section. Figure 5 represents the typical processes for the lateral waveform recorded at TAP041 station. The group-velocity dispersion of Green's function is derived using the multiple filtering techniques (Dziewonski, et al., 1969).

The station pair, approximately located on the same great circle passing through the epicenter, was chosen based on the criterion that the distance between two stations must be longer than the interested wavelength of surface waves. Thus, all of the qualified station pairs are classified into five sets across different regions (Fig. 6). Both the ray-path sets L1 and L2 are passing through the whole basin and extended to Kuanyin-Linkou area and Tanshui area, respectively. The ray-path sets L3, L4, and L5 are, however, generally within the Taipei basin. The length of ray-path for each station pair, except the set L5, is at least 10 km. The deviation angle of the propagating path direction from the great circle does not exceed 10 degrees.

Figure 7 shows the interstation phase- and group-velocity dispersion curves for every station pairs, respectively. These normal dispersion curves represent typical shape for fundamental-mode Love waves propagating through a shallow structure with low velocities in the upper stratum. For the set L1, the averaged phase velocity increases from 1.43 km/sec at a period of 2 sec to 2.55 km/sec at a period of 7 sec, and from 1.05 km/sec to 1.56 km/sec for the group velocity. However, two distinct dispersion curves with different velocities are observed for the set L2 especially along the Tanshui river basin. At each certain period in the range of interest, both of the phase and group velocities estimated from the six station pairs including site TAP041 are clearly about 0.3 km/sec slower than those are from the other ones. This
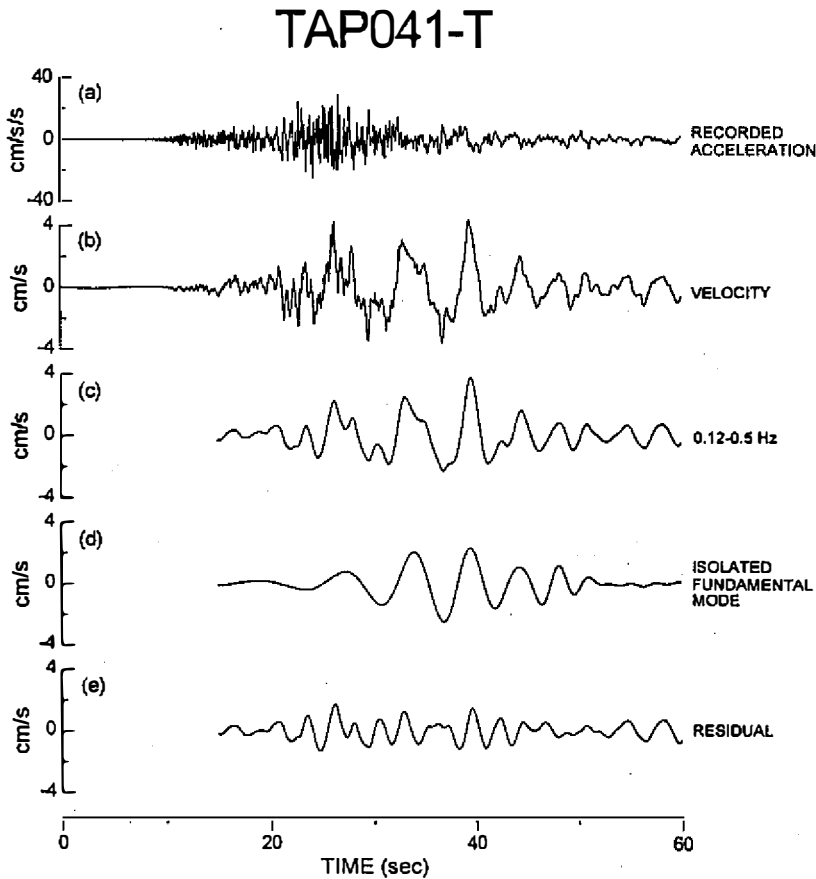
TAP041-T

Fig. 5. Depiction of data processing. They are (a) the transverse-component
acceleration seismogram recorded at station TAP041, (b) the velocity
waveform derived from integrating the record shown in (a), (c) the 0.12
– 0.5 Hz velocity waveform filtered from (b), (d) the fundamental-mode
Love wave, and (e) the residual isolated from (c) using the phase-match-
ing filter.

systematic difference is probably caused by a heterogeneous structure located along the path
toward the station TAP041, under the situation of confirmed recording time. However, all of
the paths in this set are passing through a narrow region and it is difficult to resolve such a
local lateral variation using such a long-wavelength wave. A more detailed understanding of
this pattern will required more study. On average, the phase velocity increases from 1.62 km/
sec at a period of 2 sec to 2.57 km/sec at a period of 7 sec. The group velocity increases
gradually from 1.3 km/sec to 1.5 km/sec with increasing period.

The area covered by the four interstation ray paths of set L3 basically overlap with the
paths of set L1 within and in the southeastern side of Taipei basin. The averaged phase veloc-
ity ranging from 1.43 to 2.65 km/sec is slightly faster than the one obtained from set L1. A

similar result is also shown when comparing the characteristics of dispersion curves of set L4 with that of set L2. It is suggested, by these comparisons, that the velocity beneath the region from Linkou platform to Tanshui area is lower than that within the Taipei basin in the same depth under the basement. For the set L5, considerable variation is observed among the velocities obtained from the station pairs. The short ray-path (< 10 km) could cause a large error
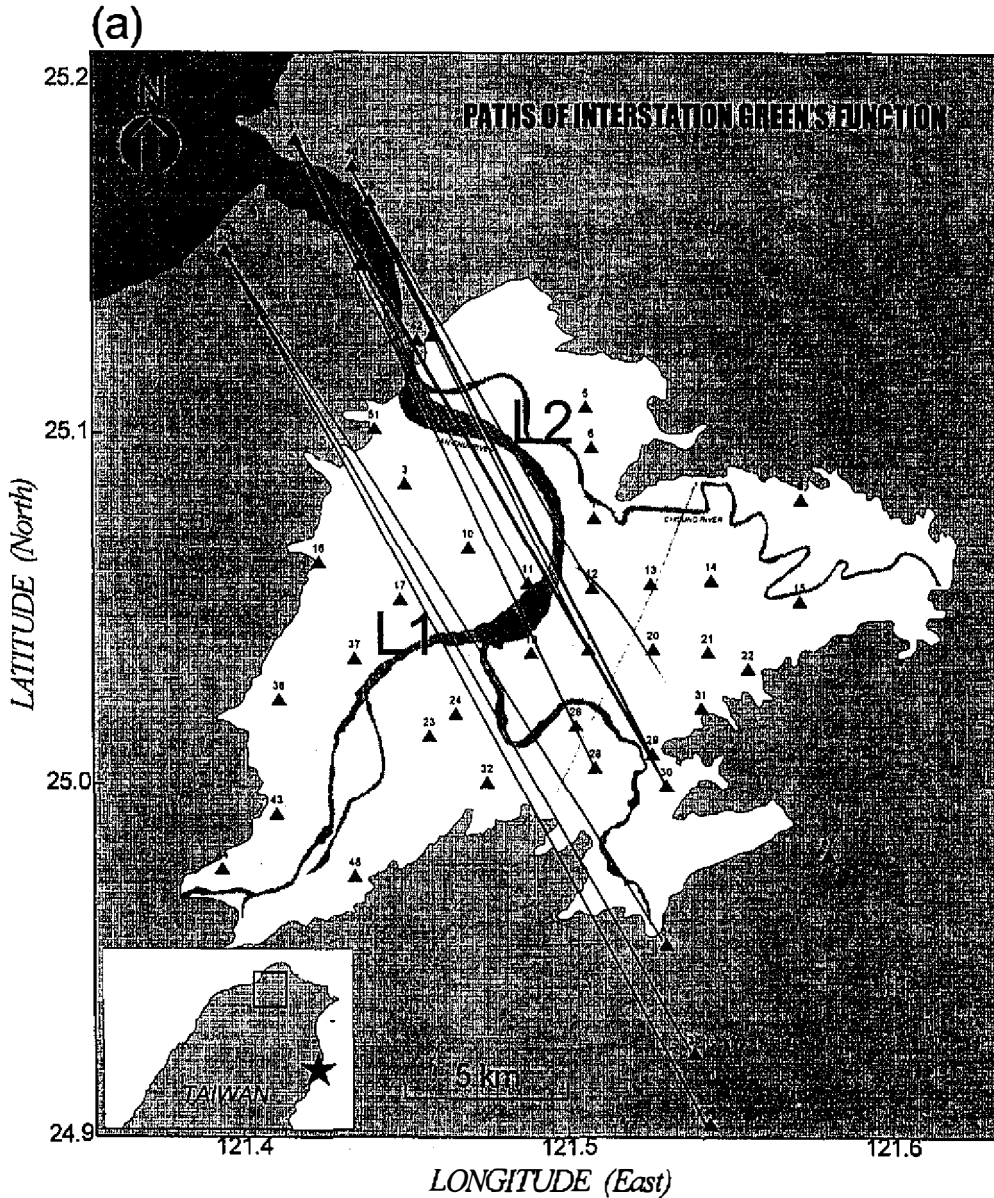
Fig. 6. Ray paths for the station pairs classified into five groups, namely, (a) L1 and L2, (b) L3, L4, and L5.
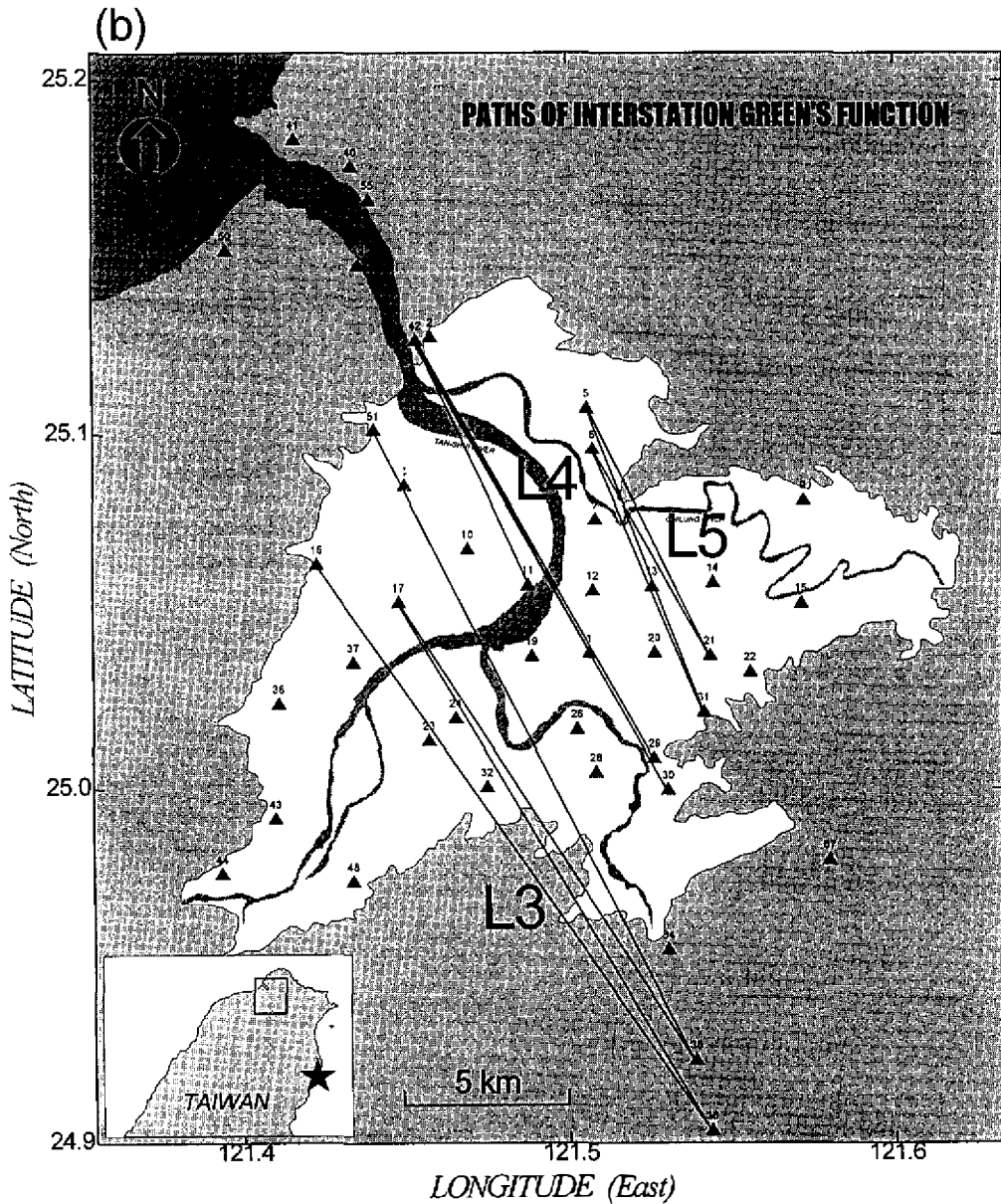
(*Fig. 6.* continued)

for estimating the phase and consequently the group velocity in the longer periods. On the other hand, the unusual uplifts in the period shorter than 2.5 sec are observed in some paths both in sets L4 and L5. Since their velocities are slow, this phenomenon is probably due to the interference of lateral multipath arrivals to the primary signals. The results of previous frequency-wavenumber analyses have provided the capability to interpret this phenomenon.

Using a standard surface-wave inversion interactive program (Russell et al., 1984), the
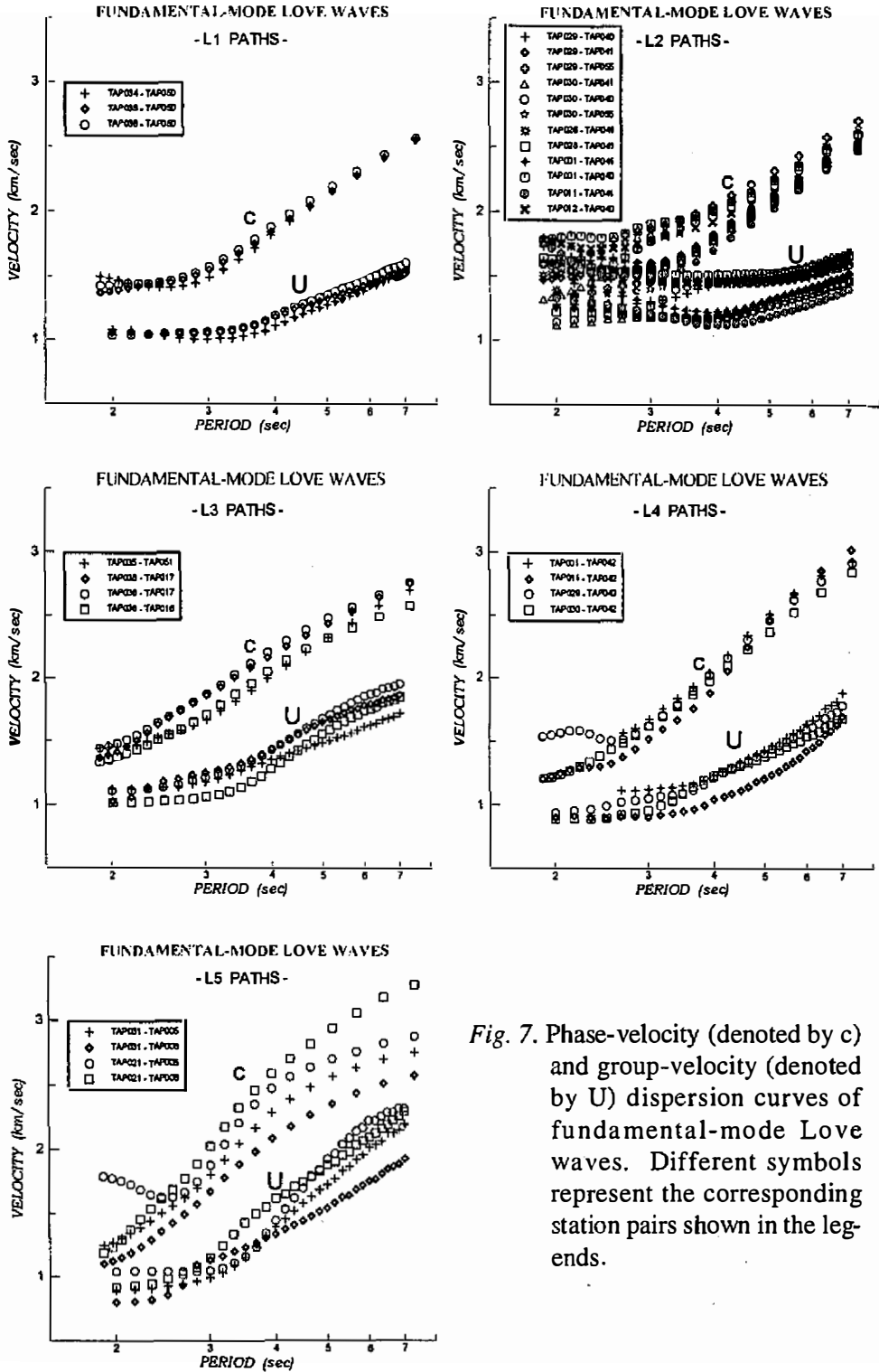
Fig. 7. Phase-velocity (denoted by c) and group-velocity (denoted by U) dispersion curves of fundamental-mode Love waves. Different symbols represent the corresponding station pairs shown in the legends.

plane-layered shear-wave velocity structure beneath the Taipei area is obtained. Here, the structure inversion is implemented by each set of ray path. The initial velocity model is composed of a set of thin layers having each layer of 500 m thickness, since there are no data for the depths of distinct velocity discontinuities at this area. The thickness of each layer is held constant during the inversion procedure. The phase- and group-velocity data are simultaneously put into the computations for obtaining best-fit theoretical dispersion curves as shown in Fig. 8. On the whole, the theoretical curves predicted by the inverted models are constrained within the standard deviations of data. The inferred shallow shear-wave structures and their averaged model from the inversion results are shown in Fig. 9 and are listed in Table 1. Considering the interested period range, the resolving ability is well for the layers of 1 to 4 km deep. Consequently, the velocities vary from 2.1 to 2.4 km/sec, which is similar to the result derived by Chen (1995) using 3-D ray-tracing inversion of body waves. Significant velocity variations of about 0.6 km/sec, however, are apparent in the substratum 1 to 2 km deep. The velocity decreases from the northeastern part to the central part of basin. Chen's (1995) results also indicated this pattern with only about 10 percent of variation, which is not evident like this article's result. It is difficult to evaluate which estimate is best, since the grid spacing used for the body-wave inversion is at least 30 km in this region. On the other hand, some inadequate path lengths are used for the surface-wave inversion, which probably cause serious error mentioned in this study. Additional data are needed to improve these estimates. Another noticeable feature is the existence of low-velocity zone in the layers from 2 to 4 km deep. When inspecting in detail both the observed and theoretical dispersion curves (Fig. 8), several fittings are not so good in the longer period range. The low-velocity layers, therefore, can be due to minor incorrect curvatures in the theoretical dispersion curves. Since our main purpose was to obtain information about preliminary structure, detailed processing was not performed to improve it, although it can be modified to a better fitting by using changeable thickness of each layer in the model during the iterative inversion.

4. DISCUSSION AND CONCLUSIONS

The subsurface stratigraphic structure of Taipei basin, in the range from the surface to several-hundred meters deep, has been explored using borehole data and reflection seismic surveys with the goal of seismic hazard mitigation. The structure under the basement plays an important role in the simulation of long-period motion of the accelerogram to predict effects on large-scale man-made structures located in the basin. Some previous studies focused on the structure investigation are generally in large scale and cannot provide a fine description for the upper part of basement. Attempts at investigating the subsurface structure in this local area using strong-motion data have not carried out often due to limitation of data. During the 1994 Nanao earthquake (M_L=6.2), the TSMIP strong-motion network in the Taipei area recorded many well-dispersed surface-wave motions, which can be used for inverting the shallow crustal structure. To utilize the strong-motion data, the consistency of the instrument timing among the network must be examined carefully. An approximate check of aligning all the P-wave travel times in the linear relationship with the respective epicentral distances was performed.
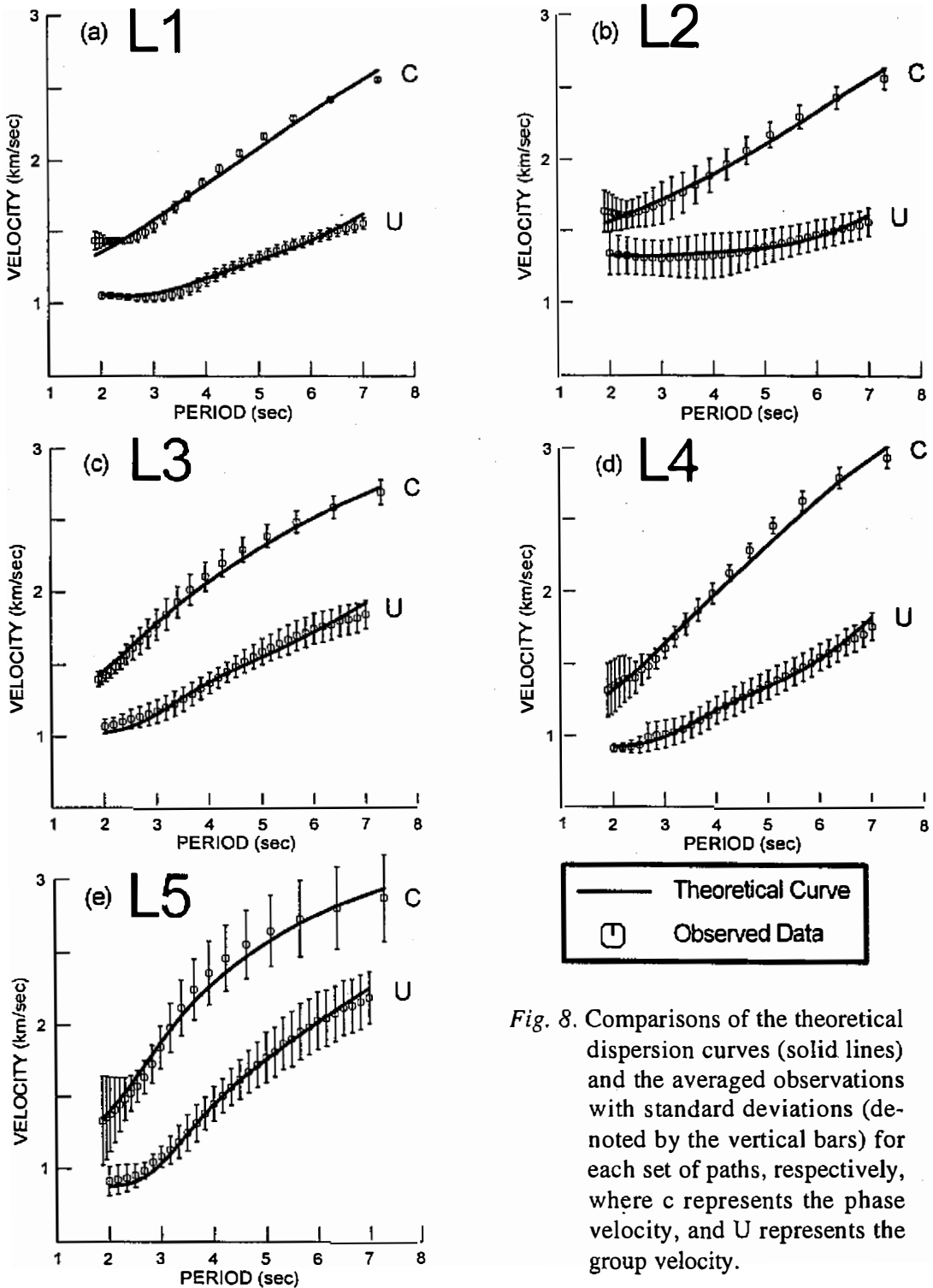
Fig. 8. Comparisons of the theoretical dispersion curves (solid lines) and the averaged observations with standard deviations (denoted by the vertical bars) for each set of paths, respectively, where c represents the phase velocity, and U represents the group velocity.
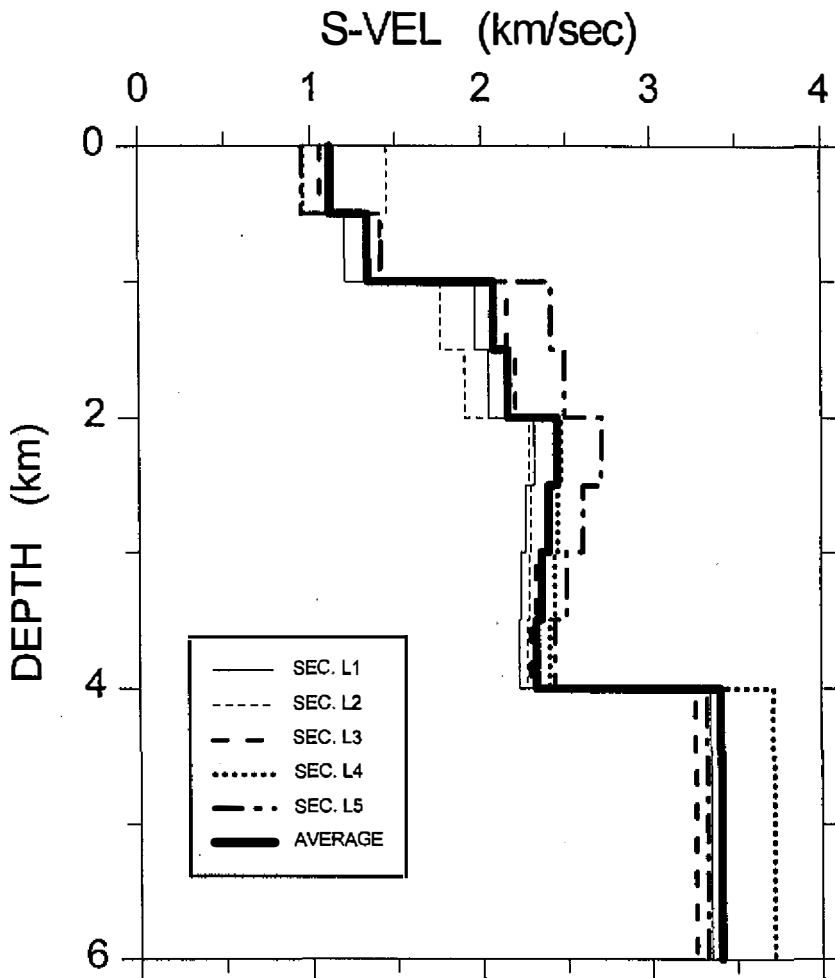
Fig. 9. Shear-wave velocity models of different paths obtained by the inversion method using the theoretical dispersion curves shown in Figure 8.

The maximum timing error of 0.3 sec for each record is expected, which corresponds to 3 percent deviation of velocity and is within the standard error for each set of data for the events studied here.

Considering the interested period range, the resolving ability is well for the layers of 1 to 4 km deep, and, consequently, the averaged shear-wave velocities varied from 2.1 to 2.4 km/ sec using the surface-wave inversion scheme. In general, the velocity decreases from the northeastern part to the central part of basin. With the considerable deviations probably due to the contamination by multipath arrivals, it is suggested that additional surface-wave data are necessary to obtain more accurate models, which can incorporate information on soil layers for better estimating the ground motions. However, the TSMIP network can record large

Table 1. S-velocity Models Obtained from Inversion of Dispersion Data for Different Ray Paths

Depth (km)	S-Velocity (km/sec) Obtained from Different Raypath Groups					Averaged S-Velocity (km/sec)	Results from Chen (1995)
	L1	L2	L3	L4	L5		
0 – 0.5	1.14	1.45	1.06	0.96	0.95	1.11 ± 0.204	
0.5 – 1.0	1.20	1.32	1.41	1.32	1.42	1.33 ± 0.089	–
1.0 – 1.5	1.96	1.76	2.15	2.06	2.41	2.07 ± 0.240	
1.5 – 2.0	2.04	1.90	2.20	2.15	2.49	2.16 ± 0.219	2.45
2.0 – 2.5	2.31	2.28	2.45	2.47	2.71	2.44 ± 0.171	
2.5 – 3.0	2.26	2.29	2.38	2.45	2.60	2.40 ± 0.136	–
3.0 – 3.5	2.23	2.28	2.32	2.43	2.50	2.35 ± 0.111	
3.5 – 4.0	2.22	2.27	2.29	2.40	2.43	2.32 ± 0.089	2.78
> 4.0	3.35	3.39	3.26	3.72	3.33	3.41 ± 0.180	

events on scale to provide data needed in engineering practices as well as for studying wave propagation. Many new and potentially fruitful studies can be launched in the future.

REFERENCES

Bloch, S., and A. L. Hales, 1968: New techniques for the determination of surface wave phase velocities. *Bull. Seism. Soc. Am.*, **58**, 1021-1034.

Campillo, M., J. C. Gariel, K. Aki, and F. J. Sanchen-Sesma, 1989: Destructive strong ground motion in Mexico City: Source, path, and site effects during great 1985 Michoacan earthquake. *Bull. Seism. Soc. Am.*, **79**, 1718-1735.

Capon, J., 1969: Signal processing and frequency-wavenumber spectrum analysis for a large aperture seismic array. MIT Lincon Laboratory, Lexington, Massachesetts.

Chen, Y. L., 1995: Three dimensional velocity structure and kinematic analysis in Taiwan area. MS Thesis of National Central University, Chung-Li, Taiwan, 172pp.

Dean, E. A., and G. R. Keller, 1991: Interactive processing to obtain interstation surface-wave dispersion. *Bull. Seism. Soc. Am.*, **81**, 931-947.

Dziewonski, A. M., S. Bloch, and M. Landisman, 1969: A technique for the analysis of transient seismic signals. *Bull. Seism. Soc. Am.*, **59**, 427-444.

Hanks, T. C., and H. Krawinkler, 1991: The 1989 Loma Prieta earthquake and its effects: Introduction to the special issue. *Bull. Seism. Soc. Am.*, **81**, 1415-1423.

Herrin, E., and T. Goforth, 1977: Phase-matched filters: Application to the study of Rayleigh waves. *Bull. Seism. Soc. Am.*, **67**, 1259-1275.

Hsieh, C. H., S. H. Hsieh, and C. W. Huang, 1996: A field survey of the Taipei basin by the shallow seismics and well loggings. Proc. of the Joint Symposium on Taiwan Quaternary (6) and on Investigation of Subsurface Geology & Engineering Environment of Taipei Basin, 52-57.

McGarr, A., M. Celebi, E. Sembera, T. Noce, and C. Mueller, 1991: Ground motion at the San Francisco international airport from the Loma Prieta earthquake sequence, 1989. *Bull. Seism. Soc. Am.*, **81**, 1923-1944.

Phillips, W. S., S. Kinoshita, and H. Fujiwara, 1993: Basin-induced Love waves observed using the strong-motion array at Fuchun, Japan. *Bull. Seism. Soc. Am.*, **83**, 64-84.

Rau, R. J., and F. T. Wu, 1995: Tomographic imaging of lithospheric structures under Taiwan. *Earth Planet. Sci. Lett.*, **133**, 517-532.

Russell, D. R., R. B. Herrmann, and H. J. Hwang, 1984: SURF: an interactive set of surface wave dispersion programs for analyzing crustal structure. *Earthquake Notes*, **55**, 13.

Shin, T. C., 1993: Progress summary of the Taiwan Strong Motion Instrumentation Program. Symposium on Taiwan strong motion instrumentation program, Central Weather Bureau, 1-10.

Shin, T. C., 1996: A study on the 1994 Nanao earthquake sequence. Report of National Science Council Research Project No. NSC85-2111-M-052-011, 62pp.

Swanger, H. J., and D. M. Boore, 1978: Importance of surface waves in strong ground motion in the period range of 1 to 10 seconds. Proc. 2nd Intern. Conf. on Microzonation, 3, 1447-1469.

Taylor, S. R., and N. Toksoz, 1982: Measurement of interstation phase and group velocities and Q using Wiener filtering. *Bull. Seism. Soc. Am.*, **72**, 73-91.

Teng, L. S., P. B. Yuan, P. Y. Chen, C. H. Peng, T. C. Lai, C. C. Lin, L. Y. Fei, and H. C. Liu, 1996: Subsurface geology of Taipei basin – New data and new viewpoint. Proc. of the Joint Symposium on Taiwan Quaternary (6) and on Investigation of Subsurface Geology & Engineering Environment of Taipei Basin, 7-10.

Teng, T. L., and J. Qu, 1996: Long-period ground motions and dynamic strain field of Los Angeles basin during large earthquakes. *Bull. Seism. Soc. Am.*, **86**, 1417-1433.

Vidale, J. E., and D. V. Helmberger, 1988: Elastic finite-difference modeling of the 1971 San Fernando, California earthquake. *Bull. Seism. Soc. Am.*, **78**, 122-141.

Wang, C. Y., W. C. Hsiao, and C. T. Sun, 1994: Reflection seismic stratigraphy in the Taipei basin (I) – Northern Taipei basin. *J. Geol. Soc. China*, **37**, 69-95.

Wang, C. Y., Y. L. Tsai, and M. L. Ger, 1995: Reflection seismic stratigraphy in the Taipei basin (II) – Western and southern Taipei basin. *J. Geol. Soc. China*, **38**, 141-172.

Wang, C. Y., Y. H. Lee, and H. C. Chang, 1996: P- and S-wave velocity structures of the Taipei basin. Symposium on Taiwan strong motion instrumentation program (II), Central Weather Bureau, 171-177.

Yamanaka, H., K. Seo, and T. Samano, 1989: Effects of sedimentary layers on surface wave propagation. *Bull. Seism. Soc. Am.,* **79**, 631-644.

Yeh, Y. H., and Y. B. Tsai, 1981: Crustal structure of central Taiwan from inversion of P-wave arrival times. *Bull. Inst. Earth Sci., Acad. Sinica,* **1**, 83-102.